Astron. Astrophys. 349, 475–484 (1999)

ASTRONOMY
AND
ASTROPHYSICS

Radio counterparts to extreme X-ray YSO's

Kester Smith[1,2], **Manuel Güdel**[2,1], **and A.O. Benz**[1]

[1] Institut für Astronomie, ETH-Zentrum, CH-8092 Zürich, Switzerland (kester, guedel, benz@astro.phys.ethz.ch)
[2] Paul Scherrer Institut, Würenlingen und Villigen, CH-5232 Villigen PSI, Switzerland

Received 26 February 1999 / Accepted 29 June 1999

Abstract. We search for radio counterparts to two recently-detected strong X-ray sources associated with highly embedded young stellar objects (SVS4/EC 95 and SVS16). We detect a radio source (S68-2) consistent with the position of EC95. We fail to detect a counterpart for SVS16, and place upper limits on its quiescent radio brightness. For S68-2, we show that the radio source has a falling spectrum, suggestive of a gyrosynchrotron emission mechanism, and that it is variable on a timescale of years. We search for, but do not detect, evidence for flaring activity on timescales of minutes to hours. We also search for, but do not detect, circular polarisation. We derive the radio luminosity and compare the object to an empirical X-ray – radio luminosity relationship established for dMe stars. We find that the object is consistent with the dwarfs relation, but is unusually X-ray rich compared to other high-luminosity coronal sources. By comparing the objects to a sample of active galactic nuclei in the L_X–L_R diagram, we rule out the possibility that either object is a background AGN. We discuss the ways in which a normal stellar coronal model might be modified to explain the strong, X-ray rich characteristics of the source, which appears to be the most extreme stellar corona yet found.

Key words: stars: activity – stars: coronae – stars: magnetic fields – stars: pre-main sequence – radio continuum: stars – X-rays: stars

1. Introduction

It is well established that young stars are often strong X-ray sources. The X-ray activity of weak-lined T Tauri stars is now regarded as a defining property of the class, and far more WTTs have been found in X-ray surveys than were known previously from other methods (Neuhäuser et al. 1995a). The Classical T Tauris (CTTS), thought to be younger than the WTTS, are also known to have associated X-ray emission, albeit less extreme. Recently, a number of younger, embedded objects have been detected in X-rays (Casanova et al. 1995, Grosso et al. 1997, Koyama et al. 1996, Carkner et al. 1998). The heating mechanism for the X-ray emitting plasma in WTTS is believed to be magnetic activity, similar to that seen on the Sun but many times stronger. This belief gains varying degrees of support from several directions. Young low-mass stars are rapidly rotating and convective, and so might be expected to have strong magnetic fields. This is borne out by direct measurements of the surface fields of several TTS (Guenther et al. 1999). Strong flaring activity is also often observed (Montmerle et al. 1983, Feigelson & Montmerle 1985, Guenther & Emerson 1997).

Preibisch (1998) (hereafter P98) reported the detection of a strong X-ray source in the Serpens star forming region. This X-ray source (hereafter Ser-X3) was identified with a group of optically invisible, IR stars collectively known as SVS4 (Strom et al. 1976). The SVS4 stars have been extensively studied in the NIR by, among others, Eiroa & Casali (1989), Eiroa & Casali (1992), Giovanetti et al. (1998) and Horrobin, Casali & Eiroa (1997). These sources are identified as pre-main sequence objects by Eiroa & Casali (1992) due to their being embedded in nebulous emission. P98 specifically associated the ROSAT source with the SVS4 member EC95, but could not exclude the possibility that nearby EC92 was the true counterpart. [Note: here, and henceforth, we use the numbering scheme of Eiroa & Casali (1992) (in their Table 1) to identify the IR sources.]. By deriving extinctions from the NIR colours, P98 calculated the hydrogen column density in the line of sight, and hence derived X-ray luminosities from the observed count rates of (2–7)$\times 10^{32}$ erg/sec in the case of EC92, or 2×10^{33} erg/sec in the case of EC95. These luminosities exceed those of the most extreme known coronal sources by an order of magnitude or more. Because there were X-ray observations at two times separated by days, and no significant variation was seen between these, P98 concluded that the emission was quiescent (i.e. non-flaring). On the basis of the extreme quiescent X-ray brightness, P98 speculated that the emission mechanism may be non-coronal.

Both IR sources are embedded in nebulosity linking them to neighbouring IR sources. This suggests they are an integral part of the SVS4 group and not background objects. Followup observations by Preibisch (1999, hereafter P99) indicate that EC95 has a total luminosity of $60 L_\odot$. The lack of a UV-ionized HII region suggests that it is a late-type star (Zhang et al. 1988). P99's IR spectroscopy shows that EC95 is K-type star. Comparison with theoretical tracks indicates that EC95 is a very young,

Send offprint requests to: K. Smith

intermediate mass star, presumably a precursor of an HAeBe star, with a mass of 1.5–5$M_{\odot}$.

IR photometry has been presented by Eiroa & Casali (1992) and Giovannetti et al. (1998), amongst others. 3mm observations by Testi & Sargent (1998) show no sign of a source at the position of EC95 (an upper limit of 2.7mJy beam^{-1} for a beam of approximately $5''\times5''$). This is consistent with the source being a HAeBe star rather than a low-mass protostar.

Preibisch (1997) (hereafter P97) used the ROSAT HRI detector to search for point sources in the NGC 1333 star-forming region. A number of X-ray sources associated with YSO's were detected. One of these X-ray sources, P97's source number 11 which we will refer to hereafter as NGC1333-X11, or just X11, was associated with the optically-invisible object SVS16. This object had a very large derived optical extinction ($A_V \sim 28$) and so appeared to have an extreme X-ray luminosity.

Preibisch et al. (1998) (hereafter PNS98) obtained further NIR photometry and spectoscopy of this object. SVS16 consists of two widely separated components, SVS16-e and SVS16-w. As with EC95, IR spectra were used with an iterative fitting technique to obtain stellar parameters. For 16-w and 16-e, the spectral types are found to be M2 and M3, the luminosities 3.8 and 2.7$L_{\odot}$ and A_V 26.2 and 28, respectively.

The X-ray luminosity was measured to be 2×10^{32} erg/sec, confirming the previous detection by P97 and suggesting that this represents the quiescent X-ray emission. PNS98 concluded that, although the X-ray source was more extreme than the most active known T Tauri star, the emission could still be explained by a coronal model as the luminosity did not exceed that of the most active RS CVn systems. PNS98 determined L_X/L_{bol}=8$\times10^{-3}$, a high value for late-type stars. From a determination of the veiling, PNS98 determined that SVS16 had little circumstellar material, and is therefore likely to be a relatively evolved YSO.

The detection of these extreme sources poses interesting questions concerning the nature of X-ray emission from pre-main sequence objects. In particular, there is the question of whether any coronal model can explain such activity. A particular problem lies with the ratio L_X/L_{bol}, which is found to be very high in each case (several $\times$ 10^{-3} for EC95). Values of L_X/L_{Bol} of more than approximately 10^{-3} are not observed for dwarf coronal sources. The correlation between L_X and rotation is instead seen to flatten off. This is attributed either to saturation of the dynamo mechanism which generates the underlying magnetic field, or to the stellar surface being completely filled with equipartition field.

There is no shortage of alternative candidates for modelling X-ray emission from a Young Stellar Object (YSO). The environments of YSO's are complex and poorly understood. Remnants of the parent cloud continue to accrete onto the star, either falling inwards in a spherically symmetric flow, or being channelled through an accretion disk. The disk may possess a magnetic field of its own, and in the case of Classical T Tauri stars (CTTS) stellar magnetic fields may play a role in channelling the material onto the stellar surface in the very inner regions (Königl 1991). At the centre of the system, the young star itself is often rapidly rotating, not yet having shed the angular momentum of its parent cloud (Bouvier et al. 1993). The interaction of various magnetic fields with the accreting material produces jets and outflows (e.g. Shu et al. 1994). Any or all of these types of processes could be invoked to produce significant X-ray flux.

The purpose of this paper is to investigate one of the empirical properties of coronae in general, that thermal X-ray emission from coronal plasma is correlated with synchrotron radio emission from accelerated electrons (Güdel & Benz 1993, Benz & Güdel 1994). We therefore search for radio counterparts to the two extreme sources. If radio luminosity of approximately the correct magnitude is found, this is evidence (although not *conclusive* evidence) that the source is coronal. Stronger evidence for magnetic activity (implying a corona) would include the detection of rapid flaring activity, circular polarization, or a synchrotron-type falling spectrum.

2. VLA archive data

Fortunately, the Serpens cloud core is an interesting area for study in the radio continuum, as it contains a number of radio jets powered by the various YSO's. A search through the literature reveals that a point-like radio counterpart to EC95 has indeed been detected by, among others, Rodríguez et al. (1980) and Snell & Bally (1986), but was not studied in much depth as these authors were more interested in spatially extended emission associated with the nearby IR source FIRS 1. Snell & Bally refer to the FIRS 1 radio counterpart as S68-1, and to the EC95 counterpart as S68-2, and we will follow this terminology. Numerous radio observations of NGC1333 also exist.

We obtained continuum observations of the SVS4 and NGC1333 regions from the Very Large Array (VLA)[1] data archive. Three data sets were obtained for SVS4. One set of A-array observations from the 20/07/95 contained both 4.9GHz and 8.4GHz data. Observations at 8.4GHz were obtained dating from the 01/05/95 (D-array) and 21/09/93 (D-C hybrid array). For NGC1333, we obtained four data sets in total. All were taken with the array in C configuration. Two observations, one at 4.9GHz and one at 8.4GHz, had been made on each of the 21st of April 1992 and the 5th of June 1992.

The radio continuum maps were reduced with the NRAO data reduction package AIPS. Standard reduction techniques were used.

3. The EC95/Ser-X3 region

The region around SVS4 contains a number of interesting radio sources. [For a detailed discussion see for example Curiel, 1995 or Rodríguez et al. 1989]. Our low-resolution D-array map is shown in Fig. 1. The positions of a number of IR sources from Eiroa & Casali (1992) have been labelled. The position of Ser X3 is also shown.

[1] The VLA is maintained by the National Radio Astronomy Observatory (NRAO). The NRAO is operated by Associated Universities Inc., under cooperative agreement with the National Science Foundation.

Table 1. The observed radio flux associated with the point-like source S68-2 (EC95) at two wavelengths on 3 separate dates. The derived radio luminosity at the distance of the Serpens cloud (310 pc) is also given, as derived from the integrated flux.

Date	ν (GHz)	Array	Peak flux (mJy)	Integrated flux (mJy)	L_R (d=310 pc, 10^{16} erg/s/Hz)
20/07/95	4.9	A	0.82±0.05	0.92±0.06	10.0±0.7
20/07/95	8.4	A	0.62±0.06	0.8±0.1	9.0±1.0
01/05/95	8.4	D	0.64±0.02	0.78±0.08	8.5±0.9
21/09/93	8.4	DnC	0.5±0.1	0.64±0.09	6.0±1.0

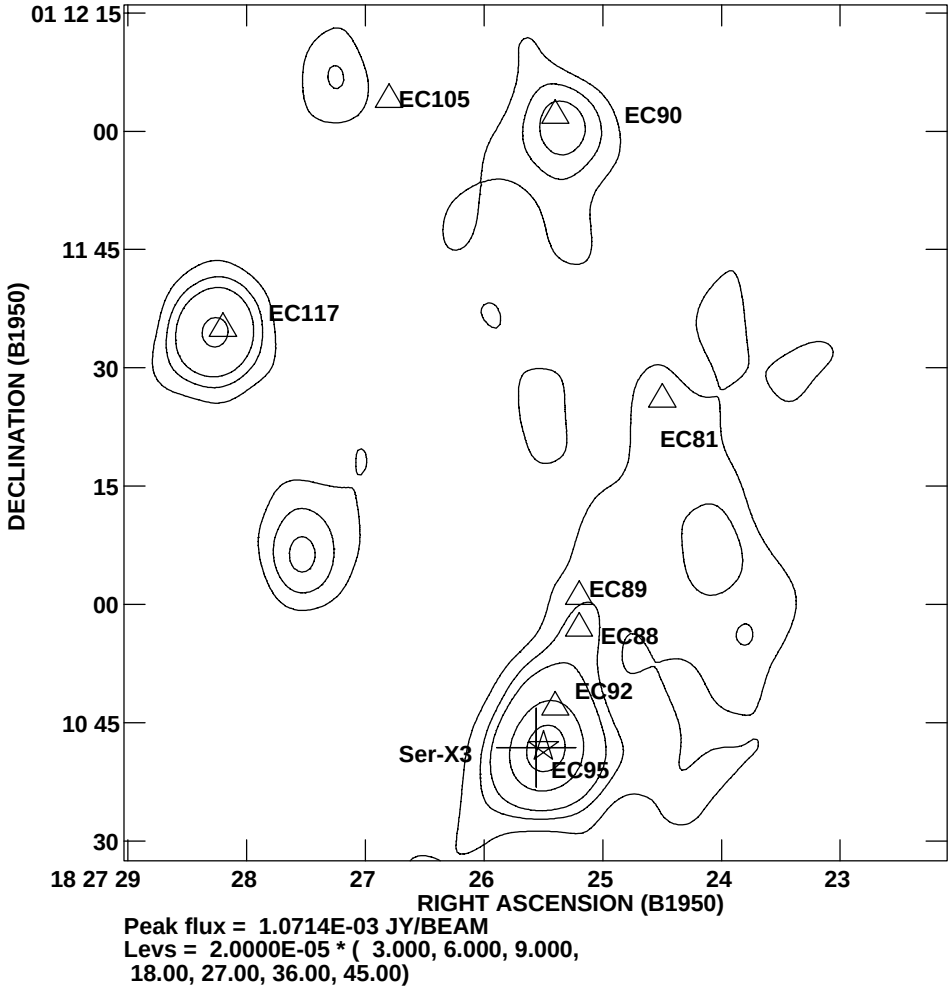

Fig. 1. D-array map of the SVS4 cluster, including EC92 and EC95. The positions of the IR sources (triangles) are taken from Eiroa & Casali (1992). These sources have been labelled with the numbers from Table 1 of Eiroa & Casali (1992). The position of the X-ray source Ser-X3 is marked by a cross, with size 10″ corresponding to the positional error given by P98. The position of EC95 is marked with a star (close to the position of the cross centre). The triangle just above this is EC92. Two other possible radio counterparts are seen, corresponding to EC117 and EC90.

A close-up view of S68-2 is provided by the A array 4.9GHz map from the 20th July 1995 (Fig. 2). The correspondence between Ser-X3 and S68-2 is clear. A clear identification can also be made between the S68-2 and the IR object EC95. Ser-X3 also correlates well with the position of EC95, as noted by P98. The coincidence of the radio source, X-ray source and IR source provides a strong case that all three detections originate for the same system. We henceforth refer to this object as EC95. We note here as an aside that a set of positions given in an earlier paper by Eiroa & Casali (1989) place the nearby IR source EC92 at a position coincident with the radio source. An earlier paper by Gómez de Castro et al. (1988), from which Eiroa & Casali (1989) obtained their positions, gives a position of EC95 and EC92 consistent with the later Eiroa & Casali (1992) paper. We conclude that the Eiroa & Casali (1992) positions as shown in Fig. 1 are correct, and that the earlier Eiroa & Casali (1989) positions are discrepant, probably because the positions of the sources can depend on the wavelength of the obserations (Gómez de Castro et al. observed in the I band, whilst Eiroa & Casali (1989) observed in the J, H and K bands).

3.1. Properties of the radio source associated with EC95

The radio fluxes for EC95 measured from our maps are shown in Table 1. Also shown are the derived radio luminosities, L_R for a distance of 310 pc (de Lara et al. 1991). From the simultaneous 4.9 and 8.4 GHz data taken on 20/07/95, we can deduce that the radio emission has a falling spectrum, $S \propto \nu^{\alpha}$ with spectral

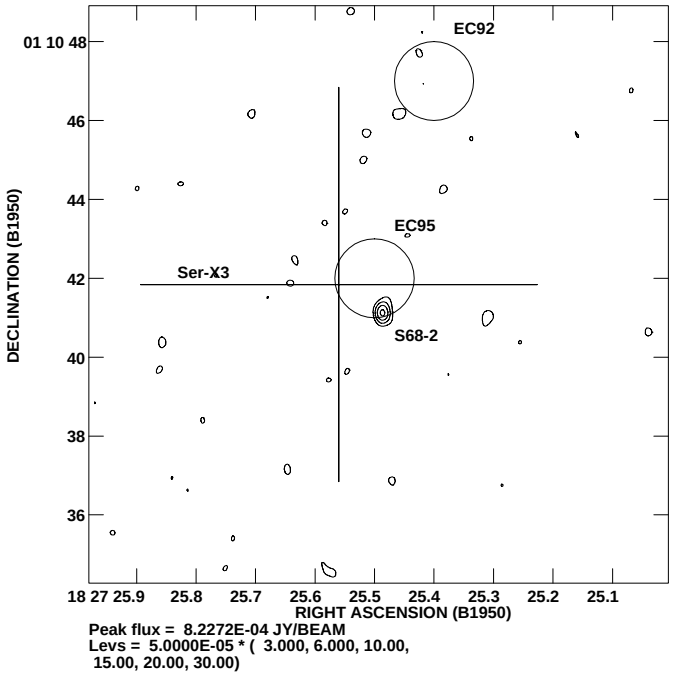

Fig. 2. A-array map of the immediate neighbourhood of S68-2 (contours). Contour levels are 3, 6, 10, 15, 20 and 30 times the RMS background (5×10^{-5}Jy). The position of the X-ray source Ser-X3 is marked by the cross. The cross is $10''$ from one side to the other, representing the quoted positional error of P98. The positions of infrared sources from Eiroa & Casali (1992) are also shown as circles whose diameters are $2''$.

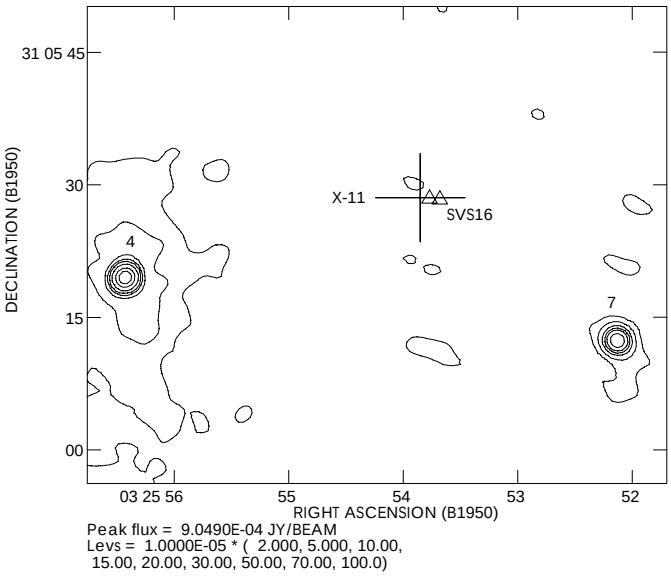

Fig. 3. Combination of four maps of the SVS16 region. Two 4.9GHz and two 8.4GHz maps have been averaged. Each map was taken with the array in C-configuration. The position of the X-ray source is marked with a cross, the size of which is $5''$. The two triangles mark the position of the east and west components of SVS16. The radio continuum sources from Snell & Bally (1986) are labelled (source 4, to the left, and source 7, to the right). The lowest contour level is twice the measured background RMS of 10 μJy. The strongest radio emission peak within the positional uncertainty of X11 had peak flux measured as 25$\pm$10 μJy, and is not a significant detection. Furthermore, its position is not consistent with the position of SVS16.

index $\alpha \approx -0.26 \pm 0.26$. The source is detected at all three dates, suggesting that the radio emission is stable, and if associated with a corona, quiescent. No significant variation is seen between the radio brightness measured on the 1st May 1995 and that measured on the 20th July, a period of approximately two-and-a-half months. The 8.4 GHz flux has varied by about 20% between 1993 and 1995, but again this is not significant. We searched for short time scale activity of S68-2 by subtracting the other sources in the field from the visibility data, and then examining the source flux as a function of time. We found no evidence of variability on time scales of minutes to hours for any of the data sets. No evidence of circular polarisation was found. We place an upper limit on the percentage circular polarisation of $V/I < 0.09$ based on the measured RMS of 0.03 mJy.

4. Search for a radio counterpart to SVS16/X11

The region around SVS16 contains several radio sources. This region was also studied by Snell & Bally (1986), and more recently by Rodríguez et al. (1999). In our data, no radio counterpart to X11 was found within the positional errors. To make a deeper search for a counterpart, the four available maps were coadded. The combined map is reproduced in Fig. 3. The position of the X-ray source (X11) is marked. The RMS of the background of the coadded map was found to be approximately 10 μJy. No strong source was seen at or close to the position of SVS16 or X11. The strongest source seen in the coadded map near the position of X11 had peak flux 25 μJy and is not significant. We therefore place a $3-\sigma$ upper limit of 30$\pm$10 μJy on the radio source, corresponding to $L_R = 4.3\times10^{15}$ erg s^{-1} Hz^{-1}.

5. X-ray properties of Ser-X3 and X11

We rederive the X-ray luminosities from the count rates given in P98 and PNS98. Our motivation is to gain values for L_X for each of the two YSO's which are directly comparable, and to derive a good estimate of the appropriate errors.

In Fig. 4, we have plotted the X-ray luminosity derived from the observed count rate as a function of hydrogen column density and temperature. It can be seen that, at such high column densities, the derived luminosity is a strong function of the extinction.

The optical extinction, A_V for each YSO has been calculated by P99 and PNS98 by fitting an IR spectrum. The optical extinction is due mostly to dust grains. The X-ray extinction is dominated by hydrogen and helium up to photon energies of about 0.5 keV (Morrison & McCammon, 1983), and is mostly due to metals at higher energies. It is relatively insensitive either to the state of the hydrogen (molecular or atomic) or to the coalescence of dust grains. There will, however, be a dependence on the relative abundances. To determine the appropriate X-ray extinction from the optical extinction, it is necessary in effect to

assume a gas-to-dust ratio. Many studies of hydrogen column density versus optical extinction have been carried out. The two quantities are usually found to be well-correlated. There are however many discrepant lines-of-sight, and there is evidence that many of the more usually quoted correlations tend to break down when the extinction becomes unusually large. In particular, the gas-to-dust ratio may be significantly lower in molecular clouds, since grain destruction mechanisms are suppressed. This has two possible implications for opacity estimates. Firstly, trapping the metals in grains can slightly increase the X-ray opacity (by about 11%) (Morrison & McCammon). Secondly, and possibly more importantly, the extinction measured by photometry (i.e. the dust extinction) would be disproportionately high compared to the true H column density. This would then lead to an overestimate of the X-ray extinction. Ultimately, the extinction along a given line of sight will be a unique parameter which should therefore ideally be derived independently for each object. This is of course rarely possible.

We have gathered together a number of typical extinction laws from the literature[2]. We have derived a mean extinction law from these of $N_H = (1.8 \pm 0.3) \times 10^{21} A_V$. Since there are so many different extinction relations, with no real basis to choose one rather than another, we treat the choice of extinction law as a source of random error.

Another uncertainty we encounter is that we do not know the plasma temperature or temperatures present. Skinner & Walter (1998) measured the spectrum of the CTTS SU Aur with ASCA, and found that the emission was dominated by a hot plasma component (which they modelled as 2.5 keV plasma), with a lesser contribution from a cooler component (kT=0.8 keV). Similar hot plasma components were seen in X-ray spectra of V773 Tau by Skinner et al. (1997). Tsuboi et al. (1998) observed V773 Tauri undergo a major flare, and detected extremely hot (up to 10 keV) plasma near the flare peak. A bimodal temperature distribution is a general feature of late-type stellar coronae. It therefore seems sensible to attempt to estimate the emission of EC95 using a two temperature model, involving a contribution from hot plasma. We use a model comprising a 1 keV and a 3 keV plasma, with equal emission measures. This model will produce a result intermediate between a pure 1 keV and a pure 3 keV model. We adopt the discrepancy between the value for 1 keV and our 50-50 model, and between the 50-50 model and the 3 keV result, as 1σ errors due to the temperature uncertainty. Finally we incorporate the error in the count rates quoted by P98 or PNS98.

For EC95, the A_V value is 36±2, so that $N_H = (6.7 \pm 1.1) \times 10^{22}$ cm^{-2}, and $L_X = 5.8\ ^{+5.4}_{-3.9} \times 10^{32}$ erg/sec (see Fig. 4).

For SVS16/X11, $A_V = 27.0 \pm 1$ (an average of 16-e and 16-w), $N_H = 5.0 \pm 0.8 \times 10^{22}$ cm^{-2}, and $L_X = 1.2\ ^{+1.1}_{-0.8} \times 10^{32}$ erg/sec.

[2] from Lada et al. (1994), Bohlin et al. (1978) (cloud sources), Jenkins & Savage (1974) (for $A_V < 1.3$), Heiles et al. (1981), Ryter (1996) and Knude & Høg (1999) (value for mixture of low and high velocity gas). We have excluded a measurement by de Geus & Burton (1991), because it is seriously discrepant from the others.

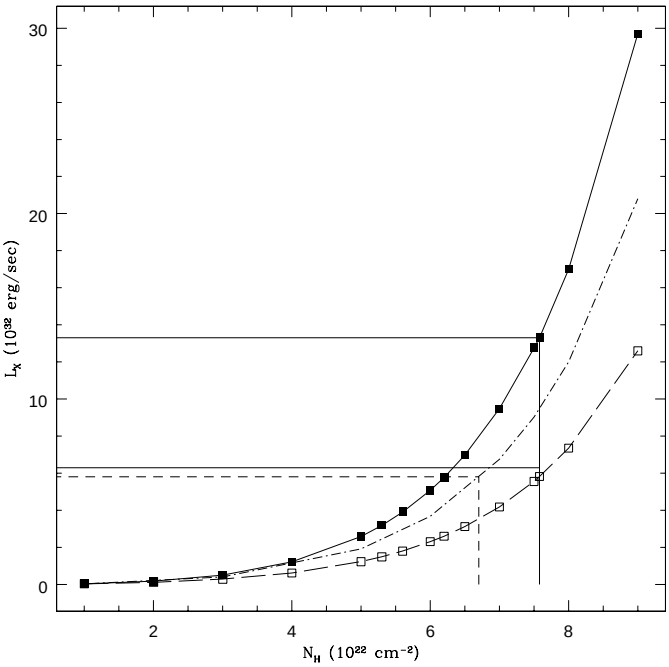

Fig. 4. L_X versus the Hydrogen column density N_H for Ser-X3/EC95. Three curves are shown, one for isothermal kT=1 keV (solid line, filled points), one for isothermal kT=3 keV (dashed line, open points), and an intermediate case for a mixture of 1 keV and 3 keV plasmas with equal emission measures (dot-dashed line). We have indicated the column density derived by P98 and the resulting X-ray luminosity (solid lines). Our values are indicated by the dashed lines. The slight discrepancy between our 3 keV curve and P98's 3 keV L_X occurs because we have used the spectral model of Mewe et al. (1995), whereas P98 used the spectral model of Raymond & Smith (1977).

5.1. Flaring versus quiescent emission

P98 concluded that Ser-X3 was a quiescent source because two observations separated by a few days both had similar X-ray fluxes. This assertion is borne out to some extent by our radio data – the source is detected at similar strength in all four of our maps. The possibility that P98 happened to observe Ser-X3 during an intense and long-lived flare, or that both P98's observations occurred during separate flare events, cannot be ruled out.

Even if we were to accept that the X-ray luminosity could, by coincidence, be due to flaring emission on two separate occasions, it seems unlikely that all the radio observations also caught Ser-X3/S68-2 in periods of enhanced activity. We consider that flaring is unlikely to explain the high X-ray luminosity of Ser-X3.

A similar situation holds for NGC1333-X11 – P97 and PNS98 obtain consistent X-ray fluxes with measurements separated by a year, and on this basis the emission appears to be quiescent.

6. Discussion

6.1. $L_X - L_R$ relation for coronal sources

There exists a correlation between X-ray and radio luminosities for active stellar coronae (Güdel & Benz, 1993), which holds for X-ray luminosities over six orders of magnitude. This relation has been established empirically, but the physical inference is that the mechanism responsible for accelerating the non-thermal electrons which emit the synchrotron radio continuum, also heat the coronal plasma which gives rise to the thermal X-ray flux. In this section, we use the radio flux we have measured in the case of EC95, and the upper limit established for any SVS16 counterpart, together with the X-ray fluxes calculated above for EC95, and given by PNS98 for SVS16, to place these objects in the L_X–L_R diagram of Güdel & Benz.

The updated X-ray–radio correlation plot of Güdel & Benz is shown in Fig. 5. A line with slope 1 has been fitted to the M-dwarfs (a subset of the crosses in the figure), as the X-ray and radio measurements are simultaneous for these objects. This relation also holds for the other low-luminosity sources – dKe stars and BY Dra objects (tidally-synchronised late-type – late-type binaries). The (mainly RS CVn binary) high-luminosity sources are systematically less X-ray bright compared to their radio luminosity. This group also includes the Weak lined T Tauri stars (WTTS). Also plotted in Fig. 5 are seven of the eight HAeBe stars detected as X-ray sources by Zinnecker & Preibisch (1994), and also observed by Skinner et al. (1993). The eighth, Z CMa, has been excluded because it was found by Skinner to be extended and so must be a wind source. Of the remaining seven, no conclusive evidence exists that they are really coronal sources. One of the detected HAeBe radio sources, TY CrA, was found by Skinner to have a falling spectrum with frequency, and so may be coronal. AB Aur was found to have a flat spectrum by Güdel et al. (1989), whilst no spectral information is available for the others. All three radio-detected HAeBe's are consistent with the population of X-ray bright stellar coronae, but not with the dwarf $L_X - L_R$ relation. Their position in the diagram lies along the radio poor edge of the high-L_X population, and this may be because their radio emission is at least in part thermal. Of the four stars with radio upper limits, two lie close to the dwarf coronal relation. One of these, HR5999, seems to have a T Tauri-type dwarf companion (Leinert et al., 1997), which may provide the coronal-type emission.

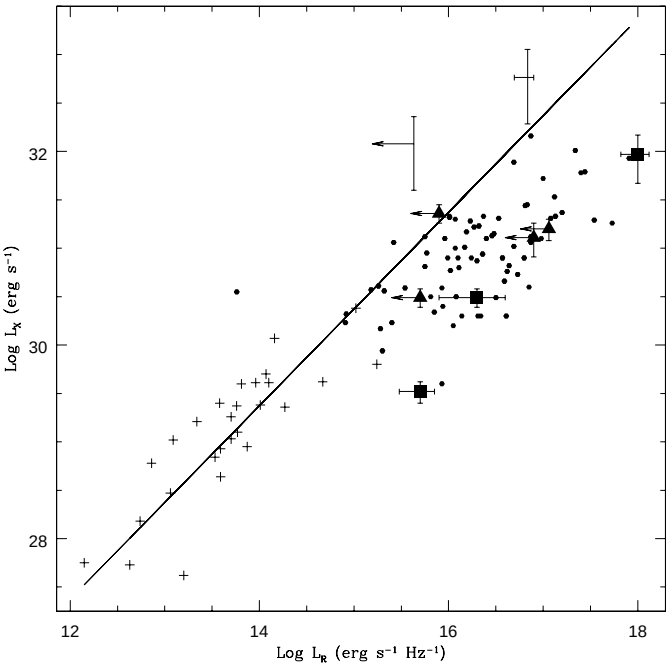

Fig. 5. The $L_X - L_R$ relation for stars, following Güdel & Benz (1993) and amended to include the X-ray luminous YSO's, and a sample of HAeBe stars. The two new YSO's are plotted with error bars only. The SVS16 point is shown with an upper limit in the radio. Both points lie significantly above the correlation line. The radio error bars for EC95 represent the range of inferred luminosities at 8.4GHz. The coronal sources have been divided into two categories. dMe stars, dKe stars and BY Dra stars, which typically have low luminosities, are plotted as crosses. WTTS, RS CVn's, Algols and FK Com stars are shown as small black dots. The best-fit line with slope 1 for the dMe stars is plotted, and extrapolated into the high-luminosity regime, for ease of comparison with the YSO points. Also shown are seven HAeBe stars, which were detected as X-ray sources by Zinnecker & Preibisch (1994) and observed in the radio by Skinner (1993). Three of the HAeBe's are detected in the radio (square points), and four are upper limits (triangles).

L_X/L_{Bol} and the problem of saturation

Studies of main-sequence dwarfs have established that there is a correlation between the rotation rate and the magnetic activity as revealed by coronal emission. This relation becomes saturated for X-ray fluxes for which $L_X/L_{Bol} > 10^{-3}$. The physical reason for this saturation could be twofold: the magnetic dynamo process becomes saturated above a certain stellar rotation rate, and/or the stellar surface becomes completely filled with equipartition field ($P_{gas} = B^2/8\pi$). The ratio L_X/L_{Bol} for the Serpens and NGC1333 YSO's is very high ($L_X/L_{Bol} \approx 5 \times 10^{-3}$ for EC95), putting the objects well into the saturation regime. It is therefore not clear if a *dwarf* coronal model could account for the X-ray emission, whether or not the sources obey the $L_X - L_R$ relation.

6.2. The nature of SVS16 – colliding winds?

The upper limit for the radio luminosity of SVS16 places it significantly above the dwarfs $L_X - L_R$ relation for dwarfs. Since even the upper limit is inconsistent with the L_X-L_R relation for dwarfs, we conclude that this object is probably not a normal stellar corona, comparable to dMe stars or to higher luminosity RS CVn or WTTS systems. We therefore consider alternative models.

Outflows are a common feature of YSO's and may provide a mechanism for generating X-ray flux without the need for magnetic fields, and thus possibly an explanation for the 'pure' X-ray source associated with SVS16.

A model in which winds from two systems collide could produce a stationary shock in which the plasma temperature could reach the required levels for thermal X-ray emission. SVS16 is known to be a wide binary, whilst the possible binarity of the components is unknown. A wind velocity of at least 400 km s^{-1} would be required to heat the plasma to about 1 keV. Typical velocities of the fast component of T Tauri outflows are 250 km s^{-1} (Hartigan et al. 1995). It is thus possible that colliding winds from two components could have a relative velocity large enough to produce such a hot shock. Mass outflow rates for T Tauri stars are found to be in the range 10^{-6} – 10^{-10} M$_\odot$ yr^{-1} (Hartigan et al. 1995). If we take a value at the high end of this range, and assume v=250 km s^{-1}, the total kinetic energy carried by the wind is then 2×10^{34} erg/sec. If the main part of the outflow is well-collimated, a near head-on collision between the outflows of two components could lead to nearly all the wind material contributing to the shock region. It is therefore energetically possible to produce the observed X-ray luminosity of X11 from such a model. For a detailed discussion of colliding wind models in YSO's see Zhekov et al., (1994).

6.3. The nature of EC95

The falling radio spectrum of EC95 is inconsistent with thermal emission from an optically thick region. For optically thick wind models, typical spectral indices of $\alpha \sim 0.6$ are expected (Wright & Barlow, 1975). We can exclude such models at the 3σ level, and conclude that the radio spectrum of EC95 is flat or falling and hence suggestive of optically thin synchrotron emission. 3mm observations by Testi & Sargent (1998) show no sign of a source at the position of EC95 (an upper limit of 2.7mJy beam^{-1} for a beam of approximately $5'' \times 5''$). This further suggests that the spectrum does not rise into the mm with an index greater than $\alpha \sim 0.5$.

Detection of circular polarization or rapid variability would both be strong evidence of a coronal-type emission mechanism. Their absence, though, does not allow us discriminate between coronal and non-coronal models.

The X-ray flux plotted for EC95 in Fig. 5 is the value calculated in Sect. 5. Although this value is lower than that given by P98, EC95 remains the most X-ray luminous object in the figure, exceeding the most luminous quiescent coronal sources by a factor of three. The source is seen to be consistent with the L_X–L_R relation for dwarfs. Note, however, that the high luminosity sources seem to be systematically X-ray poor compared to the low-luminosity sources. EC95 lies substantially above the population of high-luminosity sources, which includes the WTTS (see also for example Feigelson et al. 1998, Fig. 1).

It should be noted that there is one source amongst the high-luminosity points which also lies significantly above the correlation, and above and to the left of the general population of high-luminosity sources. This is the unusual giant-giant RS CVn system Capella (F9 III + G5 III, P=104d). The nature of Capella's corona is not well understood. No flaring behaviour is seen, and exotic coronal models have been invoked to explain the unusual properties (see for example Mewe et al., 1982, for a discussion).

Because it lies close to the dwarf relation, and because its falling-spectrum radio emission is suggestive of a synchrotron source, we conclude that EC95 is compatible with a coronal source, which can be compared to dwarf coronae.

The recent observations by P99 strongly suggest that EC95 is a proto-HAeBe star. Although intermediate-mass stars should be fully radiative, and therefore should not have a corona, previous detections of X-rays from HAeBe stars have been made (Preibisch & Zinnecker 1996, Zinnecker & Preibisch 1994). Tout & Pringle (1995) suggested that radially differential rotation in intermediate stars could lead to the formation of a temporary convective layer, and hence a corona.

An alternative explanation would be a convective low mass companion, which would supply the coronal emission.

HAeBe coronae

Very little is known about the nature of possible HAeBe coronae. Tout & Pringle (1995) showed that a HAeBe corona was energetically possible, powered by rotational shear in the rapidly spinning young object. They also estimated that the lifetime of such a corona would be of order 10^6 years, approximately the timescale for intermediate objects to evolve onto the main sequence. Lignières et al. (1996) also examined the development of convection zones in intermediate stars due to the surface torque exerted by a stellar wind, motivated largely by the need to explain chromospheric activity observed in several HAeBe stars, including AB Aur, one of the X-ray sources shown in Fig. 5.

The radio counterpart of EC95 may be compared to the corona of UV Ceti, a near-ZAMS dMe star recently observed with the VLBA at an enhanced state of activity (Benz et al. 1998). A coronal diameter of $(5.4 \pm 0.4) \times 10^{10}$ cm was measured at a radio luminosity of 8.7×10^{13} erg/sec/Hz. Scaling up the volume proportional to the observed luminosity of EC95 yields a coronal diameter of 4.8×10^{11} cm. The radius of EC95 is of order $10 R_\odot$, or 7×10^{11} cm (P99). Thus the putative corona of EC95 would not have to extend to many stellar radii in order to explain the high emission.

An interesting point arising from the $L_X - L_R$ relation of Fig. 5 is that the sources are radio poor. A possible reason for this could be an unusually high density of material in the magnetosphere. This would increase the importance of Coulomb collisions for electron energy losses (Coulomb interactions are likely to be the dominant mode of electron energy loss for *mildly* relativistic electrons in a coronal environment). This would act to limit the synchrotron radio flux. The role of increased density in limiting the radio flux whilst allowing the plasma temperature and therefore the X-ray emission to rise is thought to be important in solar microflares (Benz & Güdel, 1994).

It is apparent from Fig. 5 that the new YSO's are considerably more X-ray luminous than the existing HAeBe X-ray sources. It is tempting to speculate that the differences between EC95 and the older HAeBe stars are due to evolution of the

corona over the pre-main sequence lifetime of the stars. If the corona were to simply decay over time, we would expect the stars to move downwards and leftwards in Fig. 5, following the $L_X - L_R$ relation for dwarfs. This is possible in the case of the HAeBe upper limits. Two of these sources lie close to the dwarf relation, at lower luminosity than EC95, whilst the other two upper limits could of course have any radio luminosity up to approximately the luminosity of EC95. The three detected sources have radio luminosities comparable to EC95, but also lie some way off the coronal relation.

Companion source

The coronal emission of EC95 could be caused by a low-mass companion. This explanation is obviously attractive since low-mass pre-main sequence stars are known coronal sources. The low-mass companion would most likely be a T Tauri star. Two main classes of T Tauri star are generally identified. The Classical T Tauri stars (CTTS) accrete material from a circumstellar disk, and there may be a magnetic interaction between the stellar magnetosphere and the inner disk. The Weak lined T Tauri stars (WTTS) seem to lack disks, and so for our purposes represent the naked corona of a rapidly rotating star. It is not clear whether WTTS are more active than CTTS (Neuhäuser et al. 1995b), or not (Casanova et al. 1995, Feigelson et al., 1993). In either case, typical X-ray luminosities for T Tauri stars are significantly lower than the luminosities of EC95 and SVS16. [Some WTTS form a subset of the "high L_X sources" in Fig. 5]. Furthermore, it can be seen from Fig. 5 that EC95 is radio-poor when compared with the $L_X - L_R$ relation for dwarf coronae, and even more radio poor when compared with the X-ray bright RS CVn coronae at the top right of the graph. A further problem is that the ratio L_X/L_{bol} is large for the system as a whole. Saturation usually limits the X-ray luminosity of dwarf coronae to be at most 1–2 $\times 10^{-3}$ of the bolometric luminosity. Since a companion star would presumably contribute only a small part of the bolometric luminosity, whilst contributing most or all of the X-rays, L_X/L_{bol} would have to be very much greater than 10^{-3}. It is therefore unlikely that a low-mass companion with a normal corona could contribute the X-ray flux.

In the case of a CTTS, accretion could provide an extra heating mechanism in the magnetosphere. The pressure of accreting material arriving through a circumstellar disk can distort the magnetic field considerably (e.g. Miller & Stone 1997), rendering the field unstable to reconnection above and below the inner disk edge. Reconnection events then heat an extended corona. Higher than normal density in the magnetosphere, due to the presence of accreting material, could limit the radio flux, as discussed above. Such a model might account for both the bright X-ray emission, and the limited radio luminosity.

6.4. Background object

Finally, we consider the possibility that the X-ray and radio sources in either case might be background extragalactic objects, such as AGN or quasars. IR spectra show that EC95 and SVS16 are stellar. There remains the possibility that the X-ray/radio source has a chance coincidence with the IR object. We estimate the chance of randomly finding a radio source within 2″ of one of 160 IR sources in the 180″ radius field to be one in 50. Thus it is unlikely that the positional coincidence with EC95 is by chance. As a further step, we examine the $L_X - L_R$ relation for AGN, and compare it to that for stars, to test whether the properties of the two YSO sources might be more compatible with background extragalactic sources. In Fig. 6, we replot Fig. 5 with a sample of AGN's taken from Wolter et al. (1998) added for comparison. This sample is selected on the basis of both radio and X-ray detection, in the NRAO VLA Sky Survey (NVSS) and the ROSAT All Sky Survey (RASS) respectively. It consists mostly of Broad Emission line objects, with some radio galaxies and one candidate BL Lac object. A best-fit line with slope 1 has been determined for the AGN, and has been extrapolated into the stellar regime for comparison. Examination of a much larger sample of 800 AGN, quasars and BL Lacs shows that this relation holds for a wide range of objects (F. Bauer – personal communication). The YSO's are incompatible with this relation by three orders of magnitude. We concede that this

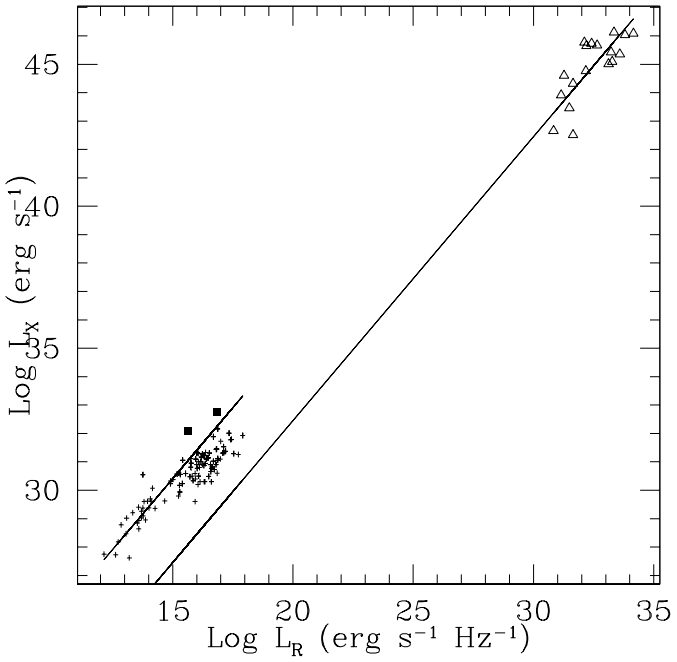

Fig. 6. $L_X - L_R$ diagram including a sample of 18 AGN (from Wolter et al. 1998). The AGN consist of 12 broad emission line objects, five radio galaxies and one BL Lac candidate. The X-ray luminosities are measured by Wolter et al. in the ROSAT 0.1–2.4 keV band and so are comparable to the YSO X-ray luminosities. The radio luminosities are given by Wolter et al. at 1.4 GHz. We have converted these luminosities to 8GHz equivalents using the relation $F_\nu \propto \nu^{-\alpha}$, where α =0.5 for broad emission line objects, 0.7 for radio galaxies and 0 for the BL Lac candidate. The best fit line with slope 1 for the M dwarfs is shown, as is the best fit line for the AGN which has been extrapolated down into the stars regime. Mistakenly taking a galactic distance for an AGN would shift it along such a line in the diagram. Both YSO points are clearly far too radio poor to be consistent with the AGN relation.

argument alone does not constitute proof that the sources are galactic. But it does demonstrate that the suggestion that the radio/X-ray sources are extragalactic does not immediately explain the anomolous $L_X - L_R$ properties.

7. Summary

We have searched for radio continuum emission associated with two extremely X-ray luminous YSO's reported by PNS98 and P97. Radio emission is expected if the source of the X-rays is coronal magnetic activity, and is furthermore expected (on empirical grounds), to obey a linear correlation. Radio emission is clearly detected in the case of EC95, but no detection was obtained for the X-ray emission associated with SVS16. For EC95, we have shown that the radio emission exhibits a falling spectrum in frequency, suggesting a synchrotron emission mechanism. We also observed some evidence of variability on time scales of years, although not on shorter time scales. We did not detect any circular polarisation, and we place a 3σ upper limit on the polarization of $V/I < 0.09$. Detection of the radio source in all our maps (together with its detection by Rodríguez et al., 1980 and Snell & Bally, 1986) suggests that this source is persistant and bears out the assertion by P98 that the emission is quiescent.

We have compared both objects on the empirical L_X–L_R relation (Fig. 5). NGC1333-X11 is inconsistent with the relation derived for the low-luminosity dMe sources. EC95 is consistent with the dMe relation, but is X-ray bright and rich compared to other high-luminosity sources, including WTTS.

We conclude that SVS16 is not likely to be an active coronal source analogous to the dMe stars. EC95 lies close to the empirical relation, and its X-ray luminosity may be due to an unusual corona. We have considered the possibility that a lower mass convective companion contributes the coronal emission in the system, but this interpretation encounters problems with the saturation effect and so is unlikely. We have investigated some ways in which standard coronal models might be modified to produce the observed properties, particularly the strong X-ray luminosity relative to the radio luminosity, and we suggest that increased density of material near the forming star could limit the radio relative to the X-ray luminosity. Future X-ray missions, such as Chandra or XMM, have the ability to measure coronal plasma properties, enabling hypotheses such as density-limited radio emission to be tested quantitatively. Finally, we note that EC95 is much more X-ray luminous than the HAeBe stars shown in Fig. 5. If at least some of the HAeBe sources are indeed coronal, we are then seeing an evolutionary picture, in which the young EC95 can be compared to the older HAeBe's. This evolutionary effect is compatible with the expectation that a corona powered by internal stellar differential rotation should decay on a timescale comparable to the pre-main sequence lifetime of these intermediate-mass stars.

Acknowledgements. We thank the data reduction staff at the VLA for their prompt and helpful responses to our data queries. We thank the referee, Thierry Montmerle, for his comments, which have helped us to significantly improve the paper.

References

Benz A.O., Güdel M., 1994, A&A 285, 621
Benz A.O., Conway J., Güdel M., 1998, A&A 331, 596
Bohlin R.C., Savage B.D., Drake J.F., 1978, ApJ 224, 132
Bouvier J., Cabrit S., Fernandez M., Martin E. L., Matthews J. M., 1993, A&A 272, 176
Carkner L., Kozak J.A., Feigelson E.D., 1998, AJ 116, 1933
Casanova S., Montmerle T., Feigelson E.D., André P., 1995, ApJ 439, 752
Curiel S., 1995, Rev. Mex. Astron. Astrofis. Serie de Conferencias 1, 59
Eiroa, Casali, 1989, A&A 223, L17
Eiroa, Casali, 1992, A&A 262, 468
Feigelson E.D., Montmerle T., 1985, ApJ 289, L19
Feigelson E.D., Casanova S., Montmerle T., Guibert J., 1993, ApJ 416, 623
Feigelson E.D., Carkner L., Wilking B.A., 1998, ApJ 494, L215
de Geus E.J., Burton W.B., 1991, A&A 246, 559
Giovanetti P., Caux E., Nadeau D., Monin J.-L., 1998, A&A 330, 990
Gómez de Castro A.I., Eiroa C., Lenzen R., 1988, A&A 201, 299
Grosso N., Montmerle T., Feigelson E.D., et al., 1997, Nat 387, 56
Güdel M., Benz A.O., Catala C., Praderie F., 1989, A&A 217, L9
Güdel M.,, Benz A.O., 1993, ApJ 405, L63
Guenther E.W., Emerson J.P., 1997, A&A 321, 803
Guenther E.W., Lehmann H., Emerson J.P., Staude J., 1999, A&A 341, 768
Hartigan P., Edwards S., Ghandour L., 1995, ApJ 452, 736
Heiles C., Stark A.A., Kulkarni S., 1981, ApJ 247, L73
Horrobin M.J., Casali M.M., Eiroa C., 1997 A&A 320, L41
Jenkins E.B., Savage B.D., 1974, ApJ 187, 243
Knude J., Høg E., 1999, A&A 341, 451
Königl A., 1991, ApJ 370, L39
Koyama K., Ueno S., Kobayashi N., Feigelson E.D., 1996, PASJ 48, 87
Lada C.J., Lada E.A., Clemens D.P., Bally J., 1994, ApJ 429, 694
de Lara E., Chavarria K.C.,, López-Molina G., 1991, A&A 243, 139
Leinert C., Richichi A., Haas M., 1997, A&A 318, 472
Lignières F., Catala C., Mangeney A., 1996, A&A 314, 465
Mewe R., Gronenschild E.H.B.M., Heise J., et al., 1982, ApJ 260, 233
Mewe R., Kaastra J.S., Liedahl D.A., 1995, Legacy 6, 16
Miller K.A., Stone J.M., 1997, ApJ 489, 890
Montmerle T., Koch-Miramond L., Flaarone E., Grindlay J.E., 1983, ApJ 269, 182
Morrison R., McCammon D., 1983, ApJ 270, 119
Neuhäuser R., Sterzik M.F., Schmitt J.H.M.M., Wichmann R., Krautter J., 1995a, A&A 295, L5
Neuhäuser R., Sterzik M.F., Schmitt J.H.M.M., Wichmann R., Krautter J., 1995b, A&A 297, 391
Preibisch T., Zinnecker H., 1996, In: Zimmermann H.U., Trümper J., Yorke H.W (eds.) Röntgenstrahlung from the Universe. MPE Report number 263, p. 17
Preibisch T., 1997, A&A 324, 690 (P97)
Preibisch T., 1998, A&A 338, L25 (P98)
Preibisch T., Neuhäuser R., Stanke T., 1998, A&A 338, 923 (PNS98)
Preibisch T., 1999, A&A 345, 583 (P99)
Raymond J.C., Smith B.W., 1977, ApJS 35, 419
Rodríguez L.F., Moran J.M., Ho P.T.P., Gottlieb E.W. 1980, ApJ 235, 845
Rodríguez L.F., Curiel S., Moran J.M., et al., 1989, ApJ 346, L85
Rodríguez L.F., Anglada G., Curiel S., 1999, ApJ, in press
Ryter C.E., 1996, Ap&SS 236, 285

Shu F.S., Najita J., Ostriker E., et al., 1994, ApJ 429, 781
Skinner S.L., Brown A., Stewart R.T., 1993, ApJS 87, 217
Skinner S.L., Güdel M., Katsuji K., Yamauchi S., 1997, ApJ 486, 886
Skinner S.L., Walter F.M., 1998, ApJ 509, 761
Snell R.L., Bally J., 1986 ApJ 303, 683
Strom S.E., Vrba F.J., Strom K.M., 1976, AJ 81, 638
Testi L., Sargent A.I., 1998, ApJ 508, 91
Tout C.A., Pringle J.E., 1995, MNRAS 272, 528
Tsuboi Y., Koyama K., Murakami H., et al., 1998, ApJ 503, 894
Wolter A., Ruscica C., Caccianiga A., 1998, MNRAS 299, 1047
Wright A.E., Barlow M.J., 1975, MNRAS 170, 41
Zhang C.Y., Laureijs R.J., Clarke F.O., 1988, A&A 196, 236
Zhekov S.A., Palla F., Myasnikov A.V., 1994, MNRAS 271, 667
Zinnecker H., Preibisch T., 1994, A&A 292, 152